

Multiplicity of $Z_{cs}(3985)$ in heavy ion collisions

L. M. Abreu

*Instituto de Física, Universidade Federal da Bahia,
Campus Universitário de Ondina, 40170-115, Bahia, Brazil*
*Instituto de Física Corpuscular, Centro Mixto Universidad de Valencia-CSIC,
Institutos de Investigación de Paterna, Aptdo. 22085, 46071 Valencia, Spain*

F. S. Navarra and M. Nielsen

*Instituto de Física, Universidade de São Paulo, Rua do Matão, 1371
CEP 05508-090, São Paulo, SP, Brazil*

H. P. L. Vieira

*Instituto de Física, Universidade Federal da Bahia,
Campus Universitário de Ondina, 40170-115, Bahia, Brazil*

Using the coalescence model we compute the multiplicity of $Z_{cs}(3985)^-$ (treated as a compact tetraquark) at the end of the quark gluon plasma phase in heavy ion collisions. Then we study the time evolution of this state in the hot hadron gas phase. We calculate the thermal cross sections for the collisions of the $Z_{cs}(3985)^-$ with light mesons using effective Lagrangians and form factors derived from QCD sum rules for the vertices $Z_{cs}\bar{D}_s^*D$ and $Z_{cs}\bar{D}_sD^*$. We solve the kinetic equation and find how the $Z_{cs}(3985)^-$ multiplicity is affected by the considered reactions during the expansion of the hadronic matter. A comparison with the statistical hadronization model predictions is presented. Our results show that the tetraquark yield increases by a factor of about 2 – 3 from the hadronization to the kinetic freeze-out. We also make predictions for the dependence of the $Z_{cs}(3985)^-$ yield on the centrality, the center-of-mass energy and the charged hadron multiplicity measured at midrapidity [$dN_{ch}/d\eta(\eta < 0.5)$].

I. INTRODUCTION

After 20 years of the $X(3872)$ observation, exotic charmonium spectroscopy is still an exciting field with discoveries every year! For recent reviews see [1–3]. As it happened in the case of ordinary light mesons, after the discovery of several new particles a pattern emerged leading to the successful $SU(3)_F$ classification scheme. Over the past two decades dozens of new hadronic states have been observed and now we need to establish connections between all the new states. An example of connection, relevant to this work, was suggested in [1], where the members of the Z_c (hidden charm states) family were grouped into the $J^P = 1^+$ Z_c nonet. This multiplet is obtained combining the well known pseudoscalar $SU(3)_F$ nonet $P = (\pi^-, \pi^0, \pi^+, K^-, K^+, K^0, \bar{K}^0, \eta, \eta')$ with a J/ψ , as shown Fig. 1. This organization of the states will eventually lead to an effective field theory of the Z_c nonet interactions with the light and heavy mesons. Such a theory is needed not only to explain the structure and spectra of these states, but also to explain their production mechanism in hadronic reactions.

The recent observation of the $X(3872)$ in $Pb - Pb$ collisions by the CMS Collaboration at the LHC [4] opened a new era for the study of the exotic charmonium states. In the beginning of these collisions, quark-gluon plasma (QGP) is formed. It then expands, cools down and hadronizes into a hot hadron gas (HG), which lives for about 10 fm and finally freezes out giving origin to the observed particles. Hadrons are formed at the beginning of the HG phase and hence interact with the (mostly light)

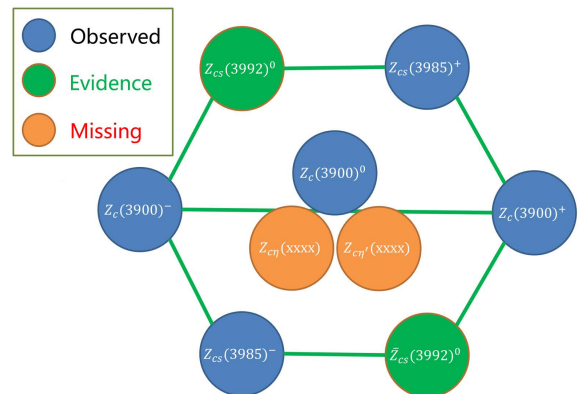


FIG. 1. $J^P = 1^+$ Z_c nonet formed by the product $P \otimes J/\psi$. Figure taken from [1].

particles in the gas. From hadronization to freeze-out the multiplicity of exotic charmonium changes because of its interactions with light hadrons. Therefore, to understand the forthcoming data it is crucial to have a reliable theory of these interactions. The $X(3872)$ has been better studied and now there are several models which describe its interactions [5–8]. The interactions of the other states are much less known. In [9] we developed an effective theory for the interactions of the $Z_{cs}(3985)^-$ with light

hadrons. In this work, we will apply it to nucleus-nucleus collisions and will compute the $Z_{cs}(3985)^-$ multiplicity which may be measured in the future.

At first sight, we might think that all the multi-quark states produced at the end of the quark-gluon plasma phase would be simply washed out during their life in the hot hadron gas. This would be specially true if these states were loosely bound meson molecules. However, our accumulated experience has shown that, in most cases, these states are easily destroyed but also easily produced. The result of this competition is unpredictable. In some cases [8, 10] the states are suppressed, in other cases their abundance remains approximately constant [11] or even grows slightly. In [12], we have shown that, in the case of the T_{cc}^+ , the time evolution of the abundance depends on the internal structure of the state: it grows if it is a compact tetraquark and drops if it is a meson molecule.

Another naive guess would be the following: if the state has a large hadronic decay width, it will be suppressed. Otherwise, it will survive the hadron gas and be observed at the end of the collision. So far this expectation has been confirmed by our calculations. Indeed, in [13] we have shown that the K^* is suppressed mainly because it decays ($K^* \rightarrow K\pi$ with a width of 50 MeV and lifetime of 4 fm) inside the hadron gas. On the other hand the abundance of D^* stays constant [14] since the decay $D^* \rightarrow D\pi$ (with a width of 70 keV) occurs only much later, after the end of the hadron gas phase. The $Z_{cs}(3985)^-$ has a decay width of 12.8 MeV, which corresponds to a lifetime of 15 fm. Since this is longer than the expected lifetime of the hadron gas, we will assume that the $Z_{cs}(3985)^-$ decays outside the hadronic fireball and will neglect the effects of its width.

In the next section, we present the $Z_{cs}(3985)^-$ (from now on simply Z_{cs}) interaction cross sections. In Section III, we discuss the details of the rate equation which governs the Z_{cs} abundance. In Section IV we show our numerical results and in the subsequent section we summarize our conclusions.

II. THE Z_{cs} INTERACTIONS

In this work we will focus on the multiplicity of the Z_{cs} produced in heavy-ion collisions. The Z_{cs} interactions with the lightest pseudoscalar mesons have been addressed in our previous work [9], where the thermal cross sections for the reactions $\bar{D}_s^{(*)}D^{(*)} \rightarrow Z_{cs}\pi$, $D^{(*)}\bar{D}^{(*)}$, $\bar{D}_sD_s^{(*)} \rightarrow Z_{cs}K$ and $\bar{D}_s^{(*)}D^{(*)} \rightarrow Z_{cs}\eta$, as well as for the inverse processes, have been calculated. In

Fig. 2 we show the lowest-order Born diagrams of the relevant processes. To calculate these cross sections, we have used an effective theory approach, with the couplings involving π , $K^{(*)}$, $D^{(*)}$ and $D_s^{(*)}$ mesons based on pseudoscalar-pseudoscalar-vector and vector-vector-pseudoscalar vertices. The couplings involving the Z_{cs} have been introduced assuming that this is a S -wave state engendered by the superposition of $D_s^{*-}D^0$ and $D_s^-D^{*0}$ configurations, with quantum numbers $I(J^P) = \frac{1}{2}(1^+)$. This can be represented by the effective Lagrangian [15],

$$\mathcal{L}_{Z_{cs}} = \frac{g_{Z_{cs}}}{\sqrt{2}} Z_{cs}^\dagger{}^\mu (\bar{D}_{s\mu}^* D + \bar{D}_s D_\mu^*), \quad (1)$$

where Z_{cs} denotes the field associated to the $Z_{cs}(3985)^-$ state. Also, the $\bar{D}_{s\mu}^* D$ and $\bar{D}_s D_\mu^*$ mean the $D_s^{*-}D^0$ and $D_s^-D^{*0}$ components, respectively.

Two aspects of the formalism developed in Ref. [9] deserve special comments. The first one concerns the effective coupling constant $g_{Z_{cs}}$, whose value has been taken from Ref. [15]. In that paper $g_{Z_{cs}}$ has been estimated to be 6.0 – 6.7 GeV assuming that the Z_{cs} is a S -wave molecule of $(\bar{D}_{s\mu}^* D + \bar{D}_s D_\mu^*)$. The second aspect refers to the empirical monopole-like form factor that has been introduced in Ref. [9] to account for the composite nature of hadrons and their finite extension and also to avoid the artificial growth of the amplitudes with the energy.

In this work we will assume that the Z_{cs} is a compact tetraquark. The interaction Lagrangian (1) is the same used to study molecular states but the coupling constant is different and can be determined with QCD sum rules (QCDSR). For a detailed discussion on this issue, we refer the reader to Ref. [16]. The advantage of using the QCDSR method is that it is more firmly rooted in QCD and also it is more appropriate to the study of multi-quark systems in a compact configuration, as it might be the case of the Z_{cs} state. In Ref. [17] a detailed analysis of the three-point correlation function of the vertices $Z_{cs}\bar{D}_s^*D$ and $Z_{cs}\bar{D}_sD^*$ was performed and the relevant form factor was numerically calculated and parametrized by the exponential function:

$$F_{Z_{cs}}(Q^2) = g_1 e^{-g_2 Q^2}, \quad (2)$$

where $Q^2 = -q^2$ is the Euclidean four-momentum of the off-shell particle (the exchanged D_s meson), $g_1 = 0.94$ GeV and $g_2 = 0.08$ GeV⁻². The coupling constant was obtained from the value of the form factor at the meson pole:

$$g_{Z_{cs}} = F_{Z_{cs}}(Q^2 = -m_{D_s}^2) = (1.4 \pm 0.4) \text{ GeV}. \quad (3)$$

We use the form factor (2) and the coupling constant (3) for the vertices $Z_{cs}\bar{D}_s^*D$ and $Z_{cs}\bar{D}_sD^*$ to calculate the cross sections of the processes displayed in Fig. 2. The

explicit expressions for the amplitudes and cross sections can be found in our previous work [9] and the resulting cross sections are shown in Fig. 3. The cross sections

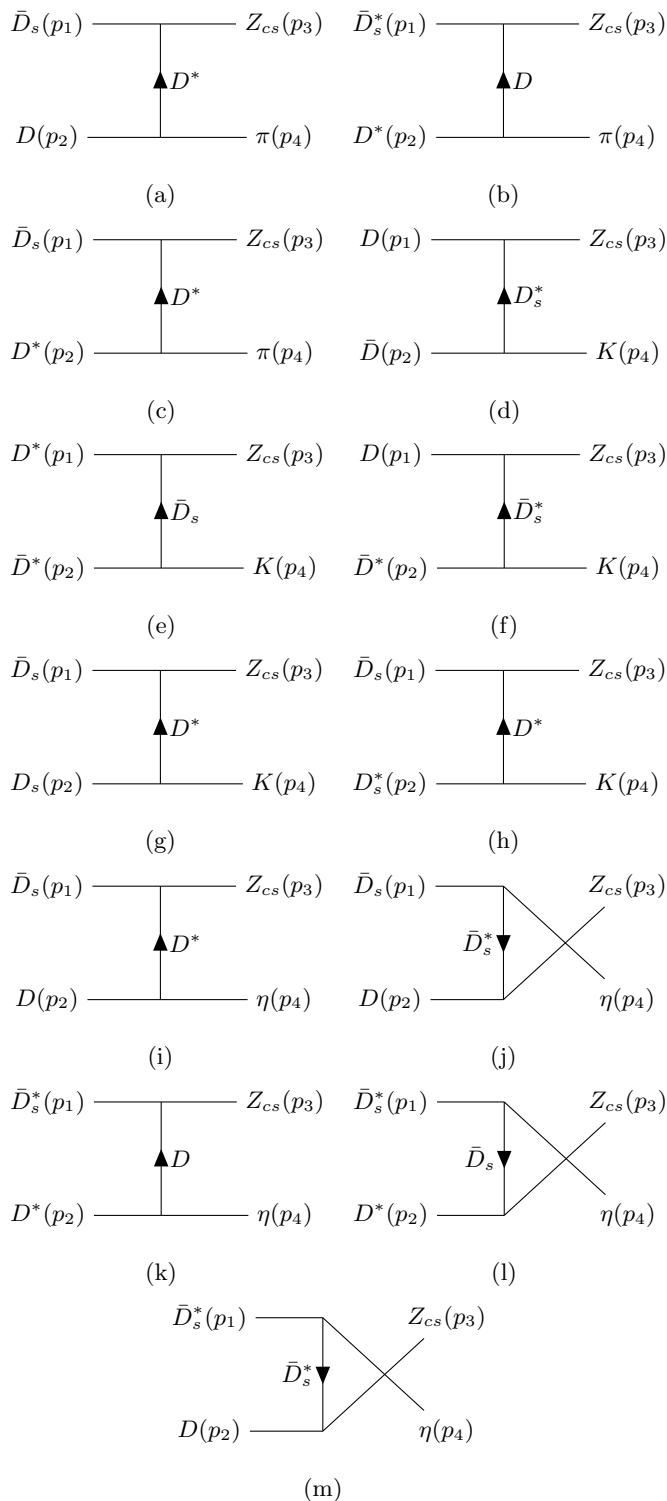


FIG. 2. Diagrams contributing to the following processes (without specification of the charges of the particles): $\bar{D}_s^{(*)} D^{(*)} \rightarrow Z_{cs} \pi$ [(a)-(c)], $D^{(*)} \bar{D}^{(*)}, \bar{D}_s D_s^{(*)} \rightarrow Z_{cs} K$ [(d)-(h)] and $\bar{D}_s^{(*)} D^{(*)} \rightarrow Z_{cs} \eta$ [(i)-(m)]. They are reproduced from Ref. [9].

obtained in [9] are different from those shown in Fig. 3. The former were obtained with monopole-like form factors and $g_{Z_{cs}} = 6.0 - 6.7$ GeV. The latter were obtained with QCDSR form factors and $g_{Z_{cs}} = 1.4$ GeV. The new cross sections are one order of magnitude smaller (than those found in [9]), they fall more slowly as the center-of-mass energy increases and they have large theoretical errors. These features can be attributed to (2), (3) and the associated errors, discussed in [17]. The QCDSR calculation can be made more precise if one includes more terms in the operator product expansion and if one has better experimental information on the Z_{cs} decays.

In the hot hadronic medium formed in heavy-ion the temperature drives the collision energy. Therefore we need to evaluate the thermally averaged cross sections (or simply thermal cross sections), defined as convolutions of the vacuum cross sections with the thermal momentum distributions of the colliding particles. For processes with a two-particle initial state going into two final particles $ab \rightarrow cd$, it is given by [5, 8, 18]:

$$\begin{aligned}
 \langle \sigma_{ab \rightarrow cd} v_{ab} \rangle &= \frac{\int d^3 \mathbf{p}_a d^3 \mathbf{p}_b f_a(\mathbf{p}_a) f_b(\mathbf{p}_b) \sigma_{ab \rightarrow cd} v_{ab}}{\int d^3 \mathbf{p}_a d^3 \mathbf{p}_b f_a(\mathbf{p}_a) f_b(\mathbf{p}_b)} \\
 &= \frac{1}{4 \alpha_a^2 K_2(\alpha_a) \alpha_b^2 K_2(\alpha_b)} \int_{z_0}^{\infty} dz K_1(z) \\
 &\quad \times \sigma(s = z^2 T^2) [z^2 - (\alpha_a + \alpha_b)^2] \\
 &\quad [z^2 - (\alpha_a - \alpha_b)^2], \tag{4}
 \end{aligned}$$

where v_{ab} denotes the relative velocity of the two initial interacting particles a and b ; $\sigma_{ab \rightarrow cd}$ represents the cross sections for the different reactions shown in Fig. 2; the function $f_i(\mathbf{p}_i)$ is the Bose-Einstein distribution of particles of species i , which depends on the temperature T ; $\beta_i = m_i/T$, $z_0 = \max(\beta_a + \beta_b, \beta_c + \beta_d)$; and K_1 and K_2 the modified Bessel functions.

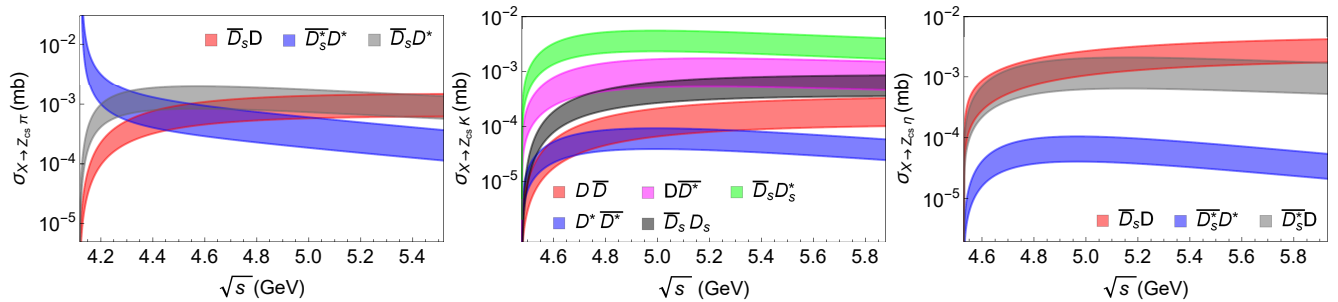


FIG. 3. Cross sections for the production processes $Z_{cs}^- \pi$ (left), $Z_{cs}^- K$ (center) and $Z_{cs}^- \eta$ (right), as functions of center-of-mass energy \sqrt{s} . The bands in the plots denote the uncertainties considered in Eq. (3).

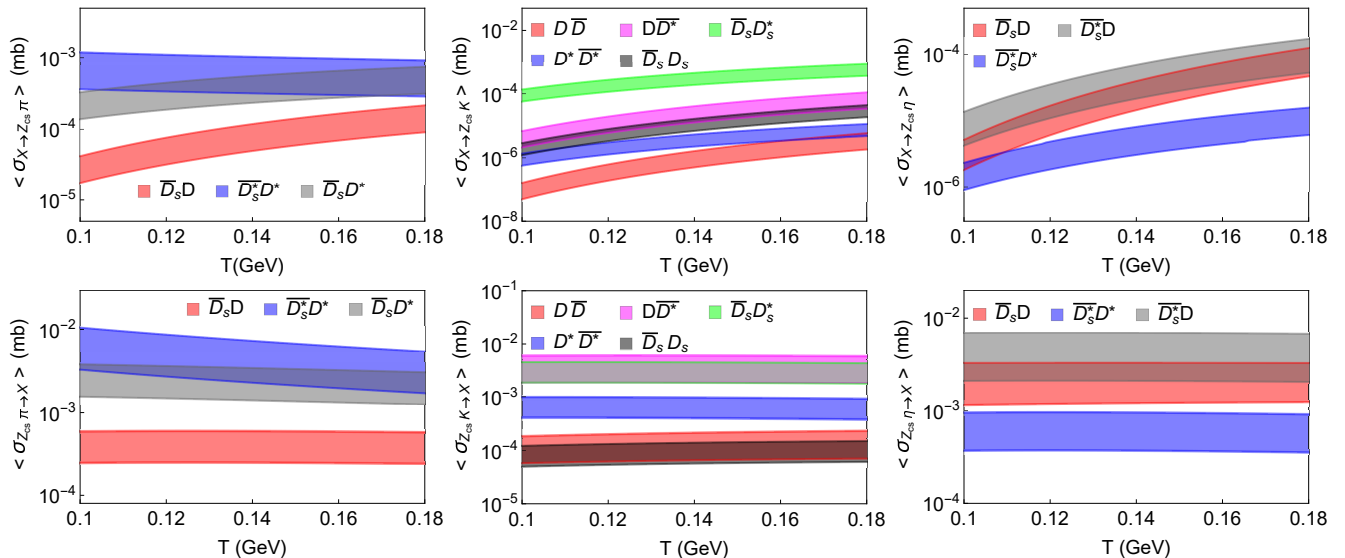


FIG. 4. Top: thermal cross sections for the production processes $Z_{cs}^- \pi$ (left), $Z_{cs}^- K$ (center) and $Z_{cs}^- \eta$ (right), as a function of temperature T . Bottom: the same as in the top panel but for the corresponding suppression processes.

In Fig. 4 we show the thermal cross sections for Z_{cs} production and absorption plotted as functions of the temperature. The results for Z_{cs} absorption have been evaluated by using the detailed balance relation. In general, the results reveal the same qualitative behavior of those discussed in [9]: the thermal cross sections for the Z_{cs} absorption do not change much in this range of temperature, staying almost constant. On the other hand, in the case of Z_{cs} production, most of the cross sections grow significantly with the temperature.

The qualitative differences between the results shown in Fig. 4 (obtained with QCDSR) and the corresponding ones reported in [9] (obtained with an empirical form factor) remain the same: the QCDSR based results are smaller than the empirical ones by one order of magnitude. In addition, the larger bands in the plots are due to the greater relative uncertainties.

Most importantly, as in [9] the thermal cross sections for Z_{cs} absorption are greater than those for production at least by one order of magnitude, depending on the tem-

perature. This result might have a considerable impact on the observed Z_{cs} multiplicity in heavy ion collisions: the initial yield at the end of the quark-gluon plasma phase might suffer significant changes during the hadron gas phase because of the interactions. This is what will be investigated in the next sections.

III. THE Z_{cs} MULTIPLICITY

A. The time evolution

We are interested in the effect of the $D_{(s)}^{(*)} D_{(s)}^{(*)} \leftrightarrow Z_{cs} \pi$, $Z_{cs} K$ and $Z_{cs} \eta$ interactions on the abundance of Z_{cs} during the hadron gas phase of heavy ion collisions. To this end, we model the time evolution of Z_{cs} multiplicity in the same way as in Ref. [12], through the momentum-

integrated rate equation [5, 8, 18]:

$$\frac{dN_{Z_{cs}}(\tau)}{d\tau} = \sum_{\substack{c,c'=D,D^* \\ \varphi=\pi,K,\eta}} [\langle \sigma_{cc' \rightarrow Z_{cs}\varphi} v_{cc'} \rangle n_c(\tau) N_{c'}(\tau) - \langle \sigma_{\varphi Z_{cs} \rightarrow cc'} v_{Z_{cs}\varphi} \rangle n_\varphi(\tau) N_{Z_{cs}}(\tau)], \quad (5)$$

where $N_{Z_{cs}}(\tau)$, $N_{c'}(\tau)$, $n_c(\tau)$ and $n_\varphi(\tau)$ are the abundances of Z_{cs} and of charmed (strange) mesons of type $c^{(\prime)}$, and the densities of charmed (strange) mesons of type $c^{(\prime)}$ and of light mesons φ at proper time τ , respectively.

In order to solve this equation we need to define the initial condition and we need to know how the quantities on the right side of the equation depend on time. This will be discussed in the next sections.

1. Medium in equilibrium

The light and heavy mesons in the medium are assumed to be in thermal equilibrium and hence $n_c(\tau)$, $n_{c'}(\tau)$ and $n_\varphi(\tau)$ can be written in the Maxwell-Boltzmann approximation as [5, 8, 18]

$$n_i(\tau) \approx \frac{1}{2\pi^2} \gamma_i g_i m_i^2 T(\tau) K_2\left(\frac{m_i}{T(\tau)}\right), \quad (6)$$

where γ_i , g_i , m_i are the fugacity, the degeneracy factor and the mass of the particle of type i , respectively. The product of the density $n_i(\tau)$ by the volume $V(\tau)$ gives the multiplicity $N_i(\tau)$.

2. Hydrodynamical expansion

The relevant quantities depend on time through the temperature $T(\tau)$ and volume $V(\tau)$, which are parametrized in order to simulate the boost invariant Bjorken expansion of the hadron gas [5, 8, 18]:

$$V(\tau) = \pi \left[R_C + v_C (\tau - \tau_C) + \frac{a_C}{2} (\tau - \tau_C)^2 \right]^2 \tau_C, \\ T(\tau) = T_C - (T_H - T_F) \left(\frac{\tau - \tau_H}{\tau_F - \tau_H} \right)^{\frac{4}{5}}. \quad (7)$$

where R_C and τ_C are the final transverse and longitudinal sizes of the QGP; v_C and a_C are its transverse flow velocity and transverse acceleration at τ_C ; T_C is the critical temperature of the quark-hadron phase transition; T_H is the temperature of the hadronic matter at the end of the mixed phase, occurring at the time τ_H ; and the kinetic freeze-out occurs at τ_F , when the temperature is T_F . We stress that the equation above is valid for $\tau \geq \tau_H$. The above parametrization is an attempt to mimic the hydrodynamic expansion of the hadronic matter. In spite of its limitations it was useful in the study of the time evolution of the multiplicity of other states (see more discussion in Refs.[5, 8]).

3. Fixing the free parameters

We will address central $Pb - Pb$ collisions at $\sqrt{s_{NN}} = 5.02$ TeV at the LHC. Following Ref. [12] the set of parameters in Eq. (7) is fixed as explained in [20] and is given in Table I. The total number of charm quarks in charmed hadrons, N_c , is conserved during the production and dissociation reactions. This is enforced by the expression $n_c(\tau) \times V(\tau) = N_c = const$, which leads to the time-dependent charm quark fugacity factor γ_c in Eq. (6). In the case of light mesons, we use their fugacities as normalization parameters to fit the multiplicities given in Table I.

TABLE I. Parameters used in Eq. (7) for the hydrodynamic expansion of the hadronic medium formed in central $Pb - Pb$ collisions at $\sqrt{s_{NN}} = 5.02$ TeV, and in Eq. (8) for the coalescence model [12, 19, 20].

| | | |
|------------------|----------------------------|-----------------------------|
| v_C (c) | a_C (c ² /fm) | R_C (fm) |
| 0.5 | 0.09 | 11 |
| τ_C (fm/c) | τ_H (fm/c) | τ_F (fm/c) |
| 7.1 | 10.2 | 21.5 |
| T_C (MeV) | T_H (MeV) | T_F (MeV) |
| 156 | 156 | 115 |
| $N_\pi(\tau_H)$ | $N_K(\tau_H)$ | $N_\eta(\tau_H)$ |
| 713 | 134 | 53 |
| N_c | $N_s(\tau_H)$ | $N_u(\tau_H)(=N_d(\tau_H))$ |
| 14 | 386 | 700 |
| m_c (MeV) | m_s (MeV) | m_q (MeV) |
| 1500 | 500 | 350 |
| ω_c (MeV) | | |
| 220 | | |

4. Initial conditions via coalescence model

The yield of the Z_{cs} state at the end of QGP is computed with the help of the coalescence model [20]. This approach is based on the overlap of the density matrix of its constituents with its Wigner function. It encodes some aspects of the intrinsic structure of the system, such as angular momentum and the type and number of constituent quarks. So, assuming that the Z_{cs} state is a S -wave tetraquark with quark content $c\bar{c}s\bar{u}$, its multiplicity at τ_C is given by [5, 8, 12, 19, 20]:

$$N_{Z_{cs}}^{coal}(\tau_C) \approx \frac{g_{Z_{cs}} [(4\pi)^3 M]^{3/2}}{(\omega^3/2V)^3} \frac{1}{(1 + 2T/\omega)^3} \\ \times \frac{N_c^2 N_s N_q}{g_c^2 g_s g_q (m_c^2 m_s m_q)^{3/2}} \quad (8)$$

where g_j and N_j are the degeneracy and number of the j -th constituent of the Z_{cs} (the index q refers to the light flavor quarks). The hadron is assumed to behave like a harmonic oscillator and the quantity ω is the oscillator

frequency. The frequency, the quark numbers and masses were taken from [12, 20] and are summarized in Table I. With the parameters from Table I Eq. (8) yields

$$N_{Z_{cs}}^{coal}(\tau_C) \approx 6.5 \times 10^{-7}. \quad (9)$$

For the sake of comparison, we compute the initial number of Z_{cs} within the Statistical Hadronization Model (SHM), which is based on Eq. (6). We find $N_{Z_{cs}}^{stat}(\tau_H) \equiv N_{Z_{cs}}(\tau_H)V(\tau_H) = 2.35 \times 10^{-3}$, which is about four orders of magnitude higher than that obtained with the coalescence model.

We emphasize that only the compact tetraquark configuration was explored. In the molecular interpretation, the oscillation frequency is estimated to be $\omega = 6B$, with B being the binding energy. However, the observed Z_{cs} mass is higher than the $D_s^{*-}D^0$ or $D_s^-D^{*0}$ thresholds, which makes it difficult to interpret the Z_{cs} as a bound state of hadrons.

B. The system size dependence

In order to express the Z_{cs} multiplicity in terms of measurable quantities, let us introduce the dependence of the $N_{Z_{cs}}$ on the system size, represented here by the measurable central value of the rapidity distribution of charged particles: $\mathcal{N} = [dN_{ch}/d\eta(|\eta| < 0.5)]^{1/3}$. To make predictions we will use empirical relations which connect the quantities listed in Table I with \mathcal{N} . The relations are briefly described below. For more details, we refer the reader to Ref. [12].

1. Kinetic freeze-out time

The empirical formula relating \mathcal{N} and the kinetic freeze-out temperature T_F is given by [12, 13]:

$$T_F = T_{F0} e^{-b\mathcal{N}}, \quad (10)$$

where $T_{F0} = 132.5$ MeV and $b = 0.02$. This parametrization has been chosen so as to fit the blastwave model analysis of the data performed by the ALICE Collaboration [21]. Inserting Eq. (10) into the Bjorken-like cooling relation $\tau_F T_F^3 = \tau_H T_H^3$, we obtain:

$$\tau_F = \tau_H \left(\frac{T_H}{T_{F0}} \right)^3 e^{3b\mathcal{N}}. \quad (11)$$

Thus, the larger (smaller) the system and the multiplicity of produced hadrons, the longer (shorter) the duration of the hadron gas. For a given system (\mathcal{N}), Eq. (11) determines the time up to which we integrate the rate equation (5). Therefore $N_{Z_{cs}}$ will be a function of \mathcal{N} .

2. Volume

We start with the relation between the volume per rapidity (dV/dy) and $dN_{ch}/d\eta$ obtained in [22] with the SHM:

$$\frac{dV}{dy} = 2.4 \left. \frac{dN_{ch}}{d\eta} \right|_{|\eta| < 0.5} = 2.4\mathcal{N}^3. \quad (12)$$

The integration over the rapidity yields the relation $V \propto \mathcal{N}^3$, with V being the chemical freeze-out volume $V_C = V(\tau_C)$. As in Ref. [20], we assume that $V_C = V_H = V(\tau_H)$. The proportionality constant can be determined using the parametrization reported in Ref. [23] for 0–5% centrality class in 5.02 TeV $Pb-Pb$ collisions. It gives the volume $V_H = 5380$ fm³ for $[dN_{ch}/d\eta(\eta < 0.5)] = 1908$ ($\mathcal{N} \approx 12.43$). Consequently, we obtain:

$$V = 2.82\mathcal{N}^3. \quad (13)$$

3. Charm quark number

As we are not aware of any experimentally established connection between N_c and $dN_{ch}/d\eta(\eta < 0.5)$ in the context of heavy ion collisions, we make use of the data from the ALICE collaboration reported in Ref. [24] on the production of charm mesons in high multiplicity pp collisions at $\sqrt{s} = 7$ TeV. The differential distribution of D mesons as a function of $dN_{ch}/d\eta$ in Fig. 2 of the mentioned paper may be parametrized by a power law, which after the integration over the appropriate interval of rapidity and transverse momentum yields the relation [12]:

$$N_D \propto \left(\frac{dN_{ch}}{d\eta} \right)^{1.6} \propto (\mathcal{N}^3)^{1.6}, \quad (14)$$

We also assume that the charm quark number and the number of D mesons are proportional:

$$N_c \propto N_D \propto (\mathcal{N}^3)^{1.6}. \quad (15)$$

The proportionality constant can then be fixed by using the number shown in Table I ($N_c = 14$ for $\mathcal{N} = 12.43$), yielding

$$N_c = 7.9 \times 10^{-5} \mathcal{N}^{4.8}. \quad (16)$$

4. Light and strange quark numbers

In the case of the light and strange quark numbers, we follow the same procedure described in the previous subsection, i.e., making use of a relation similar to Eq. (15). In the lack of data relating directly N_u, N_s to the charged particle multiplicity, we use this power law with the exponent 1 rather than 1.6, taking into account the dependence of the pions and kaons with $dN_{ch}/d\eta$ reported in

Table 3 of [21]. Next, we can fix the proportionality constants in order to match the numbers N_u, N_s displayed in Table I at $\mathcal{N} = 12.43$, obtaining the expressions

$$\begin{aligned} N_u &= 0.37 \mathcal{N}^3, \\ N_s &= 0.20 \mathcal{N}^3. \end{aligned} \quad (17)$$

5. Centrality and energy dependence

The quantity \mathcal{N} depends on the ion mass number (A) on the center-of-mass collision energy (\sqrt{s}) and on the centrality of the collision. It is interesting to find the dependence of \mathcal{N} on one of these variables, keeping the others constant. This was done in Ref. [23], where, fixing the energy at 5.02 TeV and choosing the projectiles to be $Pb - Pb$, the authors found (and displayed in their Fig. 4) a relation between \mathcal{N} and the centrality which can be parametrized as:

$$\begin{aligned} \left. \frac{dN_{ch}}{d\eta} \right|_{|\eta| < 0.5} &= 2142.16 - 85.76x + 1.89x^2 - 0.03x^3 \\ &+ 3.67 \times 10^{-5} x^4 - 2.24 \times 10^{-6} x^5 \\ &+ 5.25 \times 10^{-9} x^6, \end{aligned} \quad (18)$$

where x denotes the centrality (in %). Similarly, in the same paper we can extract the dependence of \mathcal{N} on \sqrt{s} from Fig. 3. It can be parametrized as:

$$\frac{dN_{ch}}{d\eta} = -2332.12 + 491.69 \log(220.06 + \sqrt{s}) \quad (19)$$

IV. RESULTS

A. The time evolution

Here we present our results for the time evolution of the Z_{cs} multiplicity by solving Eq. (5). We emphasize that in our calculation the Z_{cs} is treated as a compact tetraquark. This is consistent with the use of QCDSR (which are not appropriate to study extended hadron molecules) and with the choice of initial conditions given by the coalescence model with the parameters given in Table I. For the sake of comparison we will also show the results obtained with the statistical hadronization model, i.e. with Eq. (6).

In Fig. 5 we show the evolution of the Z_{cs} abundance as a function of the proper time. The band represents the uncertainties coming from the QCDSR calculations of the absorption and production cross sections. These results (obtained with initial conditions given by the coalescence model) suggest that $N_{Z_{cs}}$ increases by a factor of $\simeq 2 - 3$ during the hadron gas phase. This behavior is the result of the competition between the two contributions on the right side of the kinetic equation (5): the gain and loss terms related to the Z_{cs} -production and absorption reactions, respectively. The thermal cross sections for Z_{cs} absorption are bigger than those for Z_{cs}

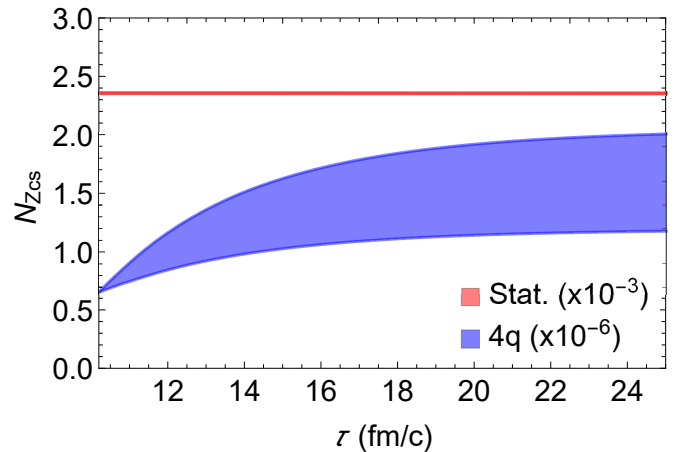


FIG. 5. Z_{cs} multiplicity as a function of the proper time in central $Pb - Pb$ collisions at $\sqrt{s_{NN}} = 5.02$ TeV. The curves represent the results obtained with initial conditions given by the coalescence and statistical hadronization models. The band denotes the uncertainties coming from the QCDSR calculations of the absorption and production cross section.

production. However, when multiplied by $N_{Z_{cs}}$ (which is initially small) they become a small number and therefore the gain term dominates, yielding a positive value for the time derivative of $N_{Z_{cs}}^{coal}$. Hence, the Z_{cs} multiplicity grows during the expansion and cooling of the system. The curve obtained with initial conditions given by the Statistical Hadronization Model remains practically constant during the hadronic gas phase. This happens because the initial value $N_{Z_{cs}}^{stat}$ is much higher than $N_{Z_{cs}}^{coal}$ and hence the loss term has the same magnitude as the gain term. It is interesting to observe that the approximate constancy of $N_{Z_{cs}}^{stat}$ is the practical definition of chemical equilibrium. In the SHM it is an assumption. Our numerical calculations give some support to it.

B. \mathcal{N} , \sqrt{s} and centrality dependence

Now we present and discuss our results for the Z_{cs} multiplicity as a function of \mathcal{N} , of \sqrt{s} and of the centrality. First we determine the \mathcal{N} -dependent initial conditions via coalescence model by substituting the relations (13), (16) and (17) into (8). These substitutions yield the relation

$$N_{Z_{cs}}^{coal} \propto \mathcal{N}^{6.6}. \quad (20)$$

Then, with the \mathcal{N} dependent initial conditions, the kinetic equation (5) was integrated up to the kinetic freeze-out time, τ_F , which, in its turn, also depends on \mathcal{N} according to Eq. (11).

The method summarized above allows us to generate the plot of the Z_{cs} abundance as a function of \mathcal{N} , shown in Fig. 6. The band representing the uncertainties is not visible here because the range of the abundances considered is much larger than in the previous figure. We

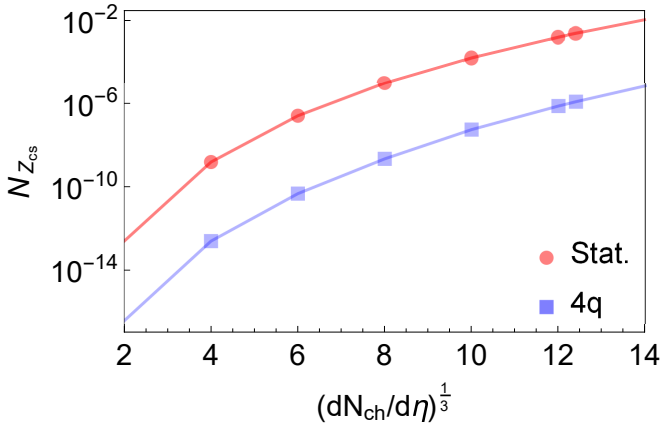


FIG. 6. The Z_{cs} multiplicity as a function of \mathcal{N} . The curves represent the results obtained with initial conditions given by the coalescence and statistical hadronization models.

observe that the multiplicity increases as the system size grows. Comparing the regions of p-p and Pb-Pb collisions (for example $\mathcal{N} \sim 2 - 3$ and $10 - 12.5$, respectively), $N_{Z_{cs}}$ changes several orders of magnitude. Both $N_{Z_{cs}}^{coal}$ and $N_{Z_{cs}}^{stat}$ show a similar behavior, but with different magnitudes. Thus, these results strongly suggest that collisions involving heavy ions appear as a very interesting environment to investigate the Z_{cs} properties and discriminate its intrinsic nature.

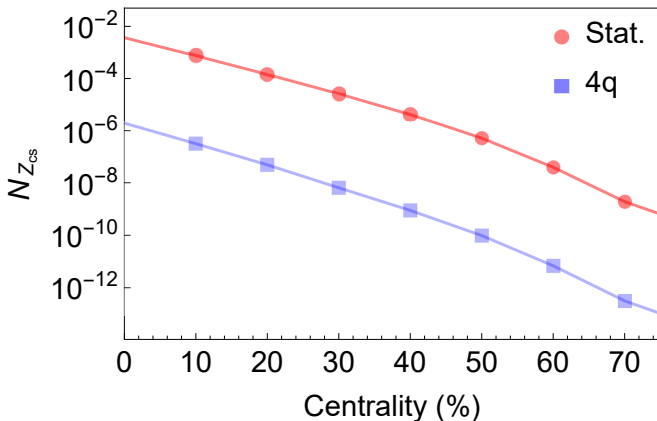


FIG. 7. The Z_{cs} multiplicity as a function of centrality in $Pb - Pb$ collisions at $\sqrt{s_{NN}} = 5.02$ TeV. The curves represent the results obtained with initial conditions given by the coalescence and statistical hadronization models.

For completeness, we show the dependence of the Z_{cs} abundance with other relevant observables. Making use of the relations (18) and (19), in Figs. 7 and 8 we present $N_{Z_{cs}}$ as a function of centrality and center-of-mass energy $\sqrt{s_{NN}}$, respectively. They show the strong dependence of the multiplicity with the centrality and $\sqrt{s_{NN}}$. The multiplicity $N_{Z_{cs}}$ increases with centrality by several orders of magnitude. In addition, our predictions for the $\sqrt{s_{NN}}$ dependence indicate that at LHC energies (i.e. 1 – 10 TeV) $N_{Z_{cs}}$ grows by one order of magnitude. We expect

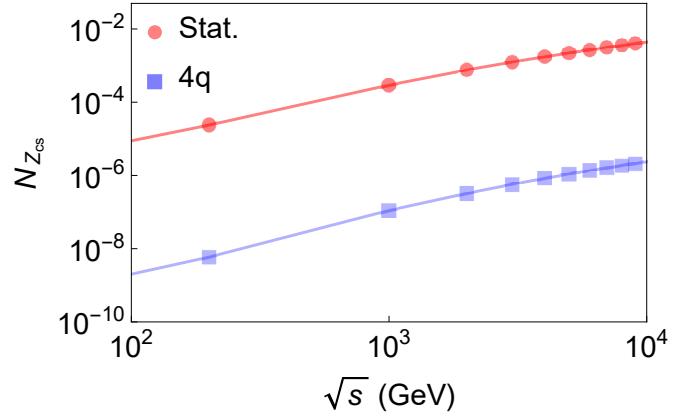


FIG. 8. The Z_{cs} multiplicity as a function of the center-of-mass energy $\sqrt{s_{NN}}$ in central $Pb - Pb$ collisions. The curves represent the results obtained with initial conditions given by the coalescence and statistical hadronization models.

that these estimates can be tested experimentally in a near future.

V. CONCLUDING REMARKS

In summary, we have improved our previous calculations [9] of the Z_{cs} cross sections, introducing QCDSR form factors and coupling constants. We have further continued the calculations, solving the rate equation and determining the time evolution of the Z_{cs} multiplicity. The main conclusion is that $N_{Z_{cs}}$ grows by a factor two during the hadron gas phase of heavy ion collisions at the LHC. Then, using a series of empirical relations connecting several variables to the measured central rapidity density, \mathcal{N} , we have made predictions for the behavior of $N_{Z_{cs}}$ with the system size, which can be confronted with data, when they are available.

This work is part of a comprehensive effort to study the behavior of all the new multi-quark states in a hadron gas. This study is of crucial importance, since in the near future these states will be investigated in relativistic heavy ion collisions. Progress has been achieved and today we certainly know more than when this program started, ten years ago. But there is much more to be done. From now on, one of the priorities will be to look for a more comprehensive approach, treating the states as members of multiplets which share common properties, instead of studying them one by one. In this sense, the classification shown in Fig. 1 is welcome.

ACKNOWLEDGMENTS

The authors would like to thank the Brazilian funding agencies for their financial support: CNPq, FAPESB and INCT-FNA.

-
- [1] C. Z. Yuan, EPJ Web Conf. **274**, 01001 (2022).
- [2] N. Brambilla, S. Eidelman, C. Hanhart, A. Nefediev, C. P. Shen, C. E. Thomas, A. Vairo and C. Z. Yuan, Phys. Rept. **873**, 1 (2020).
- [3] H. X. Chen, W. Chen, X. Liu, Y. R. Liu and S. L. Zhu, Rept. Prog. Phys. **86**, 026201 (2023).
- [4] A. M. Sirunyan *et al.* [CMS], Phys. Rev. Lett. **128**, 032001 (2022).
- [5] S. Cho and S. H. Lee, Phys. Rev. C **88**, 054901 (2013).
- [6] B. Wu, X. Du, M. Sibila and R. Rapp, Eur. Phys. J. A **57**, 122 (2021); [erratum: Eur. Phys. J. A **57**, 314 (2021)]; B. Wu, Z. Tang, M. He and R. Rapp, [arXiv:2209.13795 [hep-ph]].
- [7] A. Martínez Torres, K. P. Khemchandani, F. S. Navarra, M. Nielsen and L. M. Abreu, Phys. Rev. D **90**, 114023 (2014); [erratum: Phys. Rev. D **93**, 059902 (2016)].
- [8] L. M. Abreu, K. P. Khemchandani, A. Martínez Torres, F. S. Navarra and M. Nielsen, Phys. Lett. B **761**, 303 (2016).
- [9] L. M. Abreu, F. S. Navarra and H. P. L. Vieira, Phys. Rev. D **106**, 076001 (2022).
- [10] L. M. Abreu, F. S. Navarra and M. Nielsen, Phys. Rev. C **101**, 014906 (2020).
- [11] L. M. Abreu, F. S. Navarra, M. Nielsen and A. L. Vasconcellos, Eur. Phys. J. C **78**, 752 (2018); L. M. Abreu, K. P. Khemchandani, A. Martínez Torres, F. S. Navarra and M. Nielsen, Phys. Rev. C **97**, 044902 (2018).
- [12] L. M. Abreu, F. S. Navarra and H. P. L. Vieira, Phys. Rev. D **105**, 116029 (2022).
- [13] C. Le Roux, F. S. Navarra and L. M. Abreu, Phys. Lett. B **817**, 136284 (2021).
- [14] L. M. Abreu, F. S. Navarra and H. P. L. Vieira, Phys. Rev. D **106**, 074028 (2022).
- [15] Q. Wu and D. Y. Chen, Phys. Rev. D **104**, 074011 (2021).
- [16] L. M. Abreu, F. S. Navarra, M. Nielsen and H. P. L. Vieira, Eur. Phys. J. C **82**, 296 (2022).
- [17] J. M. Dias, X. Liu and M. Nielsen, Phys. Rev. D **88**, 096014 (2013).
- [18] P. Koch, B. Müller and J. Rafelski, Phys. Rep. **142**, 167 (1986).
- [19] L. M. Abreu, Phys. Rev. D **103**, 036013 (2021);
- [20] S. Cho *et al.* [ExHIC], Prog. Part. Nucl. Phys. **95**, 279 (2017).
- [21] B. Abelev *et al.* [ALICE Collaboration], Phys. Rev. C **88**, 044910 (2013).
- [22] V. Vovchenko, B. Dönigus and H. Stoecker, Phys. Rev. C **100**, 054906 (2019).
- [23] H. Niemi, K. J. Eskola, R. Paatelainen and K. Tuominen, Phys. Rev. C **93**, 014912 (2016).
- [24] J. Adam *et al.* [ALICE], JHEP **09**, 148 (2015).